Ultra-sensitive and Wide Bandwidth Thermal Measurements of Graphene at Low Temperatures

K.C. Fong[1] and K.C. Schwab[1]

Applied Physics, Caltech, Pasadena, CA 91125 USA

Abstract

Graphene is a material with remarkable electronic properties[1] and exceptional thermal transport properties near room temperature, which have been well examined and understood[2, 3]. However at very low temperatures the thermodynamic and thermal transport properties are much less well explored[4, 5] and somewhat surprisingly, is expected to exhibit extreme thermal isolation. Here we demonstrate an ultra-sensitive, wide-bandwidth measurement scheme to probe the thermal transport and thermodynamic properties of the electron gas of graphene. We employ Johnson noise thermometry at microwave frequency to sensitively measure the temperature of the electron gas with resolution of $4mK/\sqrt{Hz}$ and a bandwidth of 80 MHz. We have measured the electron-phonon coupling from 2-30 K at a charge density of $2 \cdot 10^{11} cm^{-2}$. Utilizing bolometric mixing, we have sensed temperature oscillations with period of 430 ps and have determined the heat capacity of the electron gas to be $2 \cdot 10^{-21} J/(K \cdot \mu m^2)$ at 5 K which is consistent with that of a two dimensional, Dirac electron gas. These measurements suggest that graphene-based devices together with wide bandwidth noise thermometry can generate substantial advances in the areas of ultra-sensitive bolometry[6], calorimetry[7], microwave and terahertz photo-detection[8], and bolometric mixing for applications in areas such as observational astronomy[9] and quantum information and measurement[10].

Given the single atomic thickness and low electron density, the electron gas of graphene is expected to be very weakly coupled to surrounding thermal baths at low temperatures. Figure 1b shows the temperature dependence of the expected cooling channels for the two-dimensional electron gas: cooling through electron diffusion, $G_{\rm WF}$, emission of phonons, $G_{\rm ep}$, and emission of photons, $G_{\rm rad}$, where $G_{\rm tot}$ the sum of all three mechanisms. Electron diffusion is expected to follow the usual Wiedemann-Franz form: $G_{\rm WF} = L_0 T_e/R$, where L_0, k_B, and R are the Lorentz constant, the Boltzmann constant, and the electrical resistance of the sheet, respectively. The thermal conductance through the emission of blackbody photons into the electrical measurement system (Johnson noise) is limited by the quantum of thermal conductance,[11] $G_0 = \pi k_B^2 T_e/(6\hbar)$ and the bandwidth of the connection to the environment, B: $G_{\rm rad} = G_0(2\pi\hbar B/k_B T_e)$, assuming $B < k_B T_e/(2\pi\hbar)$ which is the bandwidth of the black body radiation[12–14].

The electron gas can thermalize through the emission of acoustic phonons[16–19]. For temperatures below the Bloch-Grüneisen temperature[15, 20, 21] ($T_{BG} = 2c\pi^{1/2}\hbar v_F n^{1/2}/(v_F k_B) = 33$ K for $n = 10^{11}$ cm^{-2}), heat transport between electrons and phonons[22] is expected to follow $\dot{Q} = A\Sigma(T_e^4 - T_p^4)$, where A is the sample area, $\Sigma = (\pi^{5/2} k_B^4 D^2 n^{1/2})/(15\rho\hbar^4 v_F^2 c^3)$ is the coupling constant, D is the deformation potential, $v_F = 10^6$ m/s is the Fermi velocity, c = 20 km/s is the speed of sound, and n is the charge carrier density. When $|T_e - T_p| \ll T_p$, $G_{\rm ep} = 4\Sigma A T^3$. Through careful engineering of the sample geometry and the coupling to the electrical environment, it is possible to force the heat through the phonon channel, minimizing $G_{\rm tot}$ (see supplementary information) and at very low temperatures, this thermal conductance is expected to be extraordinarily weak[19] (Fig. 1).

Furthermore, the heat capacity of the electron gas is expected to be minute[19]: $C_e = (2\pi^{3/2} k_B^2 n^{1/2} T_e)/(3\hbar v_F)$. At 100 mK and with $n = 10^{11}$ cm^{-2}, one expects $C_e = 2.3 \cdot k_B$ for a $1\mu m$ x $1\mu m$ flake. This combined with the thermal conductance, one can estimate the thermal time constant: $\tau = C_e/G_{\rm tot}$. Assuming $G_{\rm tot} \approx G_{\rm ep}$, one expects the maximum thermal time constant to be $\tau = 10ps$ at 10K, $1ns$ at 1K, and $10\mu s$ at 10mK. Due to the linear bands of graphene, and the correspondingly high Fermi temperature, the heat capacity of graphene can be 50 times lower than that of a heterostructure 2DEG, assuming $n = 10^9$ cm^{-2}.

Given the expected very weak coupling and high speed thermal response, we have imple-

mented microwave frequency noise thermometry to explore these delicate and high bandwidth thermal properties, (Fig.1). Noise thermometry has shown itself to be an excellent and nearly non-invasive probe of electron temperature for nanoscale devices [7, 11] with very minimal back-action heating. Using a superconducting LC matching network, we match the relatively high impedance of a 15 $\mu m \times 6.8\ \mu m$ flake of graphene, 30 $k\Omega$ at the charge neutrality point (CNP), to a 50 Ω measurement circuit; the network resonates at 1.161 GHz with a bandwidth of 80 MHz. This allows for fast, high sensitivity measurements of the electron gas temperature which follows the Dicke Radiometer formula[23]: $\Delta T_e/(T_e + T_S) = (Bt_m)^{-1/2}$, where t_m is the measurement time, and $T_S = 12$ K is the system noise temperature of our cryogenic HEMT amplifier. This leads to a temperature resolution of $\sqrt{S_T} = 4mK/\sqrt{Hz}$ at a sample temperature of 2 K. Much lower system noise temperatures are possible with the use of high bandwidth, nearly quantum-limited SQUID amplifiers[24].

Our graphene sample is fabricated using exfoliation onto a Si wafer coated with 285 nm of SiO; the single layer thickness is confirmed using Raman spectroscopy[25]. Ohmic contact is made using evaporated Au/Ti leads. Figure 1e shows the measured noise spectrum in band of the HEMT amplifier showing the Johnson noise thermometry of the sample. Given the sample size and the electrical resistance, we expect the thermal conductance to be dominated by $G_{\rm ep}$ for temperatures above 300 mK. At lower temperatures, superconducting leads can be used to block transport through $G_{\rm WF}$ [11].

By applying currents through the graphene sample and producing ohmic heating, $\dot{Q}$, we can measure the thermal conductance of the electron gas. We impose a small oscillating current bias at 17.6 Hz, detect the resulting 35.2 Hz temperature oscillations of the electron gas in the limit where $\Delta T_e/T_e \simeq 10^{-2}$, and then compute the differential thermal conductance: $G = \dot{Q}/\Delta T_e$ (Fig. 2b). This data is well fitted with the expected form: $G = 4\Sigma A T^p$, with Σ and p as fitting parameters. At the CNP where $n = 2 \cdot 10^{11}$ cm^{-2} due to impurities, we find $\Sigma = 0.07\ W/(m^2K^3)$ which is consistent with a deformation potential of $D = 47$ eV, and a power law of $p = 2.7 \pm 0.3$ The power law exponent is near the theoretical expectation of $p = 3$ and the deformation potential is within the range of previous measurements[17, 20, 21, 26].

Figure 2 also shows the results of applying a wide range of DC current biases, where T_e can be much larger than T_p. We find this data to fit the expected form: $T_e = (\dot{Q}/(A \cdot \Sigma) + T_p^{p+1})^{1/(p+1)}$ using Σ and p found from the differential measurements. Finally, we applied

a heating signal at 1.161 GHz, at the frequency of our LC matching network where the microwave absorption into the graphene is nearly complete (Fig. 1d), and measured the increase in the electron gas temperature with the Johnson noise. This method also shows the same thermal conductance and demonstrates graphene as a bolometer to microwave frequency radiation.

To probe the thermal time constant, τ, and reveal the heat capacity of the graphene, we utilize the microwave frequency impedance matching network together with the small temperature dependence of the electrical resistance of graphene (Fig. 1c). We first apply a high frequency oscillating current, within the impedance matching band to heat the sample: $\dot{Q} = I_{heat}^2(t) \cdot R(T_e) = I_{heat}^2 R(T_e)(1 + cos(2\omega_{heat}t))/2$ where $\omega_{heat} = 2\pi \cdot 1.161$ GHz. Similar to above thermal conductance measurements, the DC component of the temperature change is observed through the Johnson noise of the sample. If the thermal time constant of the graphene electron gas satisfies $2\omega_{heat}\tau < 1$, then the temperature of the sample will oscillates at $2 \cdot \omega_{heat} = 2\pi \cdot 2.322$ GHz. From our measurement of the $G_{\rm ep}$ and our expectation of the heat capacity , we expect $2\omega_{heat}\tau = 1$ for $T = 5.7$ K. Given the weak dependence of the sample resistance on temperature, $dR/dt =\sim 400\Omega/K$ at 4 K, the impedance, $Z(\omega)$, will also oscillate at $2\omega_{heat}$ with T_e. By applying a second smaller modulation tone at $\omega_{mod} = \omega_{heat} - 1$ kHz, the impedance oscillations are transduced into a very small voltage oscillation, typically 10-100 pV, and are mixed back into the range of our matching network: $\delta V(t) = (I_{mod}e^{-i\omega_{mod}t}) \cdot (\delta Z e^{-i2\omega_{heat}t})$, where a component of $\delta V(t)$ oscillates at $2\omega_{heat} - \omega_{mod}$. See supplementary information for more details of the mixing and signal processing.

For temperatures above 5 K we observe this mixed tone, resulting from bolometric mixing, with its amplitude agreeing with our expectations, demonsrating the temperature oscillations of the graphene sheet at 2.322 GHz. However, for temperatures below 5 K we observe a substantial decrease in the amplitude of the mixed tone, consistent with the expected roll-off due to the finite thermal response time of the sheet due to the heat capacity. At 5.25 K, we calculate a heat capacity of 12,000 k_B which is comparable to the smallest heat capacity measured to date[8].

The data we have gathered on the thermal transport and thermodynamic properties of graphene from 2-30 K and the sensitivity of our wide bandwidth thermometry system motivates an estimation of the sensitivity of graphene as a bolometer and photon detector at lower temperatures[27]. Figure 4 shows the expected sensitivity as a bolometer versus noise

bandwidth for various temperatures, where the noise equivalent power (NEP) is given by: $NEP = G_{\rm tot} \cdot \sqrt{S_T}$, where S_T is the noise spectral density of noise thermometer. Given the minute heat capacity for T < 1K, the temperature resolution is expected to be limited by the thermodynamic fluctuations of the energy of the electron gas [27, 28]: $\langle \Delta T_e^2 \rangle = k_B T_e^2 / C$, which gives $S_T(\omega) = 4\tau k_B T_e^2 / (C(1+(\tau\omega)^2))$. The maximum sensitivity versus measurement bandwidth is result of the balance between gaining resolution in the noise thermometry by increasing the measurement band, and increasing the thermal response by decreasing $G_{\rm rad}$. As is clear from the plots, a graphene-based bolometer may exceed the sensitivity of the current state of the art bolometers developed for far-infrared/submillimeter wave astronomy with a sensitivity of $6 \cdot 10^{-20} W/\sqrt{Hz}$ and a thermal time constant of τ = 300 ms [6], an improvement in bandwidth of ∼5 orders of magnitude.

As a photon detector and calorimeter, the expected energy resolution if given by[7, 27]: $\Delta E = NEP \cdot \sqrt{\tau}$. Given the exceptionally fast thermal time constant, one expects single photon sensitivity to gigahertz photons(Fig. 4.) For astrophysical applications in terahertz spectroscopy, one expects an energy resolution of one part in 1000 at 300 mK for an absorbed 1 THz photon. This satisfies the instrument resolution requirements for future NASA missions (BLISS) at 3He-refrigerator temperatures[9]. At 10mK, the intriguing possibility to observe single 500MHz photons appears possible.

Furthermore, for high rates of photon flux, $\dot{n}$, the quantization of the field produces shot noise on the incoming power: $S_{shot} = 2(\hbar\omega)^2 \dot{n}\ W^2/Hz$. For sufficiently high rates of microwave photons, this noise will dominate the temperature fluctuations of the sample. At 100 mK, and with 10 GHz photons, for fluxes greater than 10^6 photons/s the noise of the bolometer should be dominated by the shot noise of the microwave field. In this way, graphene would act as a photodetector for microwaves: square law response, absorptive, and sensitive to the shot noise of the incoming field. We know of no other microwave detector which has these characteristics and would open the door to novel quantum optics experiments with microwave photons.

Note: During the writing of this work, we have become aware to two other experimental works which touch on some these concepts [29, 30].

K.C.F developed these concepts, measurement and sample designs, fabricated devices, and performed data collection and analysis. K.C.S instigated the work, developed these concepts, and over saw the work.

We acknowledge help with microfabricated LC resonators from M. Shaw, and helpful conversations with P. Kim, J. Hone, E. Hendrickson, J. P. Eisentien, A. Clerk, P. Hung, E. Wollman, A. Weinstein, B.-I. Wu, D. Nandi, J. Zmuidzinas, J. Stern, W. H. Holmes, and P. Echternach. This work has been supported by the the FCRP Center on Functional Engineering Nano Architectonics (FENA) and US NSF (DMR-0804567). We are grateful to G. Rossman for the use of a Raman spectroscopy setup. Device fabrication was performed at the Kavli Nanoscience Institute (Caltech) and at the Micro Device Laboratory (NASA/JPL).

The authors declare that they have no competing financial interests.

Correspondence and requests for materials should be addressed to K.C.S (email: schwab@caltech.edu).

[1] Castro Neto, A. H., Guinea, F., Peres, N. M. R., Novoselov, K. S., & Geim, A. K. The electronic properties of graphene. *Rev. Mod. Phys.* **81**, 109 (2009).

[2] Balandin, A. A., Ghosh, S., Bao, W., Calizo, I., Teweldebrhan, D., Miao, F. & Lau, C. N. Superior thermal conductivity of single-layer graphene. *Nano Lett.* **8**, 902 (2008).

[3] Seol, J. H., Jo, I., Moore, A. L., Lindsay, L., Aitken, Z. H., Pettes, M. T., Li, X., Yao, Z., Huang, R., Broido, D., Mingo, N., Ruoff, R. S. & Shi, L. Two-dimensional phonon transport in supported graphene. *Science* **328**, 213–216 (2010).

[4] Zuev, Y. M., Chang, W. & Kim, P. Thermoelectric and Magnetothermoelectric Transport Measurements of Graphene. *Phys. Rev. Lett.* **102**, 096807 (2009).

[5] Wei, P., Bao, W., Pu, Y., Lau, C. N. & Shi, J. Anomalous Thermoelectric Transport of Dirac Particles in Graphene. *Phys. Rev. Lett.* **102**, 166808 (2009).

[6] Kenyon, M., Day, P., Bradford, C., Bock, J. & Leduc, H. Electrical properties of background-limited membrane-isolation transition-edge sensing bolometers for far-ir/submillimeter direct-detection spectroscopy. *J. Low Temp Phys.* **151**, 112–118 (2008).

[7] Roukes, M. Yoctocalorimetry: phonon counting in nanostructures. *Physica B* **263-264**, 1–15 (1999).

[8] Wei, J., Olaya, D., Karasik, B. S., Pereverzev, S. V., Sergeev, A. V. & Gershenson, M. E. Ultrasensitive hot-electron nanobolometers for terahertz astrophysics. *Nature Nano.* **3**, 496 (2008).

[9] Benford, D.,Amato, M.,Mather, J.,Moseley, S. & Leisawitz, D. Mission concept for the single aperture far-infrared (SAFIR) observatory. *Astrophys. Space Sci.* **294**, 177–212 (2004).

[10] Rocheleau, T., Ndukum, T., Macklin, C., Hertzberg, J. B.,Clerk, A. A. & Schwab, K. C. Preparation and detection of a mechanical resonator near the ground state of motion. *Nature* **463**, 72 (2010)

[11] Schwab, K., Henriksen, E., Worlock, J. & Roukes, M. Measurement of the quantum of thermal conductance. *Nature* **404**, 974–977 (2000).

[12] Pendry, J. Maximun information flow. *J. Phys. E* **16**, 2161–2171 (1983).

[13] Meschke, M., Guichard, W. & Pekola, J. Single-mode heat conduction by photons. *Nature* **444**, 187–190 (2006).

[14] Schmidt, D. R., Schoelkopf, R. J. & Cleland, A. N. Photon-Mediated Thermal Relaxation of Electrons in Nanostructures. *Phys. Rev. Lett.* **93**, 045901 (2004).

[15] Hwang, E. H. & Das Sarma, S. Acoustic phonon scattering limited carrier mobility in two-dimensional extrinsic graphene. *Phys. Rev. B* **77**, 115449 (2008).

[16] Tse, W.-K. & Das Sarma, S. Energy relaxation of hot Dirac fermions in graphene. *Phys. Rev. B* **79**, 235406 (2009).

[17] Bistritzer, R. & MacDonald, A. H. Electronic cooling in graphene. *Phys. Rev. Lett.* **102**, 206410 (2009).

[18] Kubakaddi, S. S. Interaction of massless dirac electrons with acoustic phonons in graphene at low temperatures. *Phys. Rev. B* **79**, 075417 (2009).

[19] Viljas, J. K. & Heikkilä, T. T. Electron-phonon heat transfer in monolayer and bilayer graphene. *Phys. Rev. B* **81**, 245404 (2010).

[20] Chen, J.-H., Jang, C., Xiao, S., Ishigami, M., & Fuhrer, M. S. Intrinsic and extrinsic performance limits of graphene devices on SiO_2. *Nature Nano.* **3**, 206 (2008).

[21] Efetov, D. K. & Kim, P. Controlling electron-phonon interactions in graphene at ultra high carrier densities. *Phys. Rev. Lett.* **105**, 256805 (2010).

[22] Roukes, M., Freeman, M. R., Germain, R. S. & Richardson, R. C. Hot electrons and energy transport in metals at millikelvin temperatures. *Phys. Rev. Lett.* **55**, 422 (1985).

[23] Dicke, R. H. Measurement of Thermal Radiation at Microwave Frequencies. *Rev. Sci. Inst.* **17**, 268 (1946).

[24] Mück, M., Welzel, C. & Clarke, J. Superconducting quantum interference device amplifiers at gigahertz frequencies. *Appl. Phys. Lett.* **82**, 3266–3268 (2003).

[25] Ferrari, A. C. Raman Spectrum of Graphene and Graphene Layers. *Phys. Rev. Lett.* **97**, 187401 (2006).

[26] Bolotin, K. I., Sikes, K. J., Hone, J., Stormer, H. L., & Kim, P. Temperature-dependent transport in suspended graphene. *Phys. Rev. Lett.* **101**, 096802 (2008).

[27] Mather, J. C. Bolometer noise: nonequilibrium theory. *Applied Optics* **21**, 1125–1129 (1982).

[28] Chui, T. C. P., Swanson, D. R., Adriaans, M. J., Nissen, J. A. & Lipa, J. A. Temperature fluctuations in the canonical ensemble. *Phys. Rev. Lett.* **69**, 3005–3008 (1992).

[29] Vora, H.,Kumaravadivel, P.,Nielsen, B. & Du, X. Bolometric response in graphene based superconducting tunnel junctions. *preprint arXiv:1110.5623.*

[30] Yan, J.,Kim, M.-H.,Sushkov, A. B.,Jenkins, G. S., Milchberg, H. M., Fuhrer, M. S. & Drew, H. D. Dual-gated bilayer graphene hot electron bolometer. *preprint arXiv:1111.1202*.

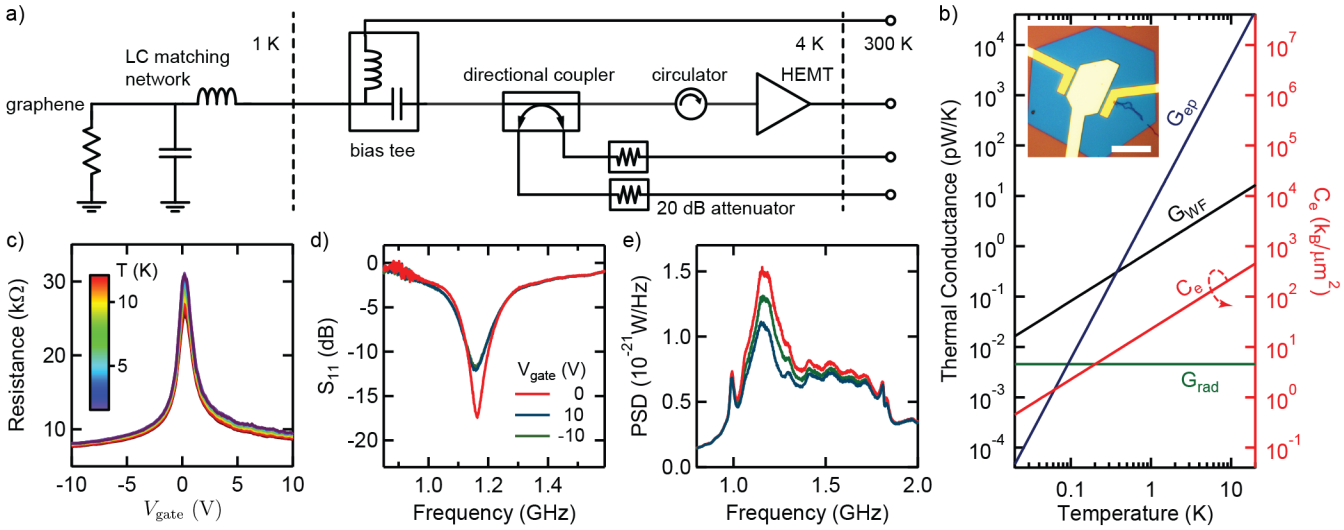

FIG. 1: **A** shows the measurement circuit: graphene, impedance matched with 1.161 GHz resonant, lithographic LC network (NbTiN film, $T_c = 13.5$ K), and connected to HEMT amplifier. **B** shows the expected thermal conductances ($G_{\rm WF}$, $G_{\rm ep}$, $G_{\rm rad}$) and heat capacity versus temperature for assuming a bandwidth of 80 MHz, $n = 10^{11}$ cm^{-2}, and $A = 10^{-10}$ m^2. The inset shows an optical micrograph of the graphene sample. Scale bar is 15 μm long. **C** shows the two-terminal resistance of the graphene vs gate voltage, taken from 1.65-12 K. **D** shows the reflected microwave response versus gate voltage. The absorption dip at 1.161 GHz shows that the graphene is well matched to 50 Ω in a 80 MHz band. **E** shows spectra of the measured noise power taken at various sample temperatures, demonstrating the Johnson noise signal of the graphene in the impedance matching band.

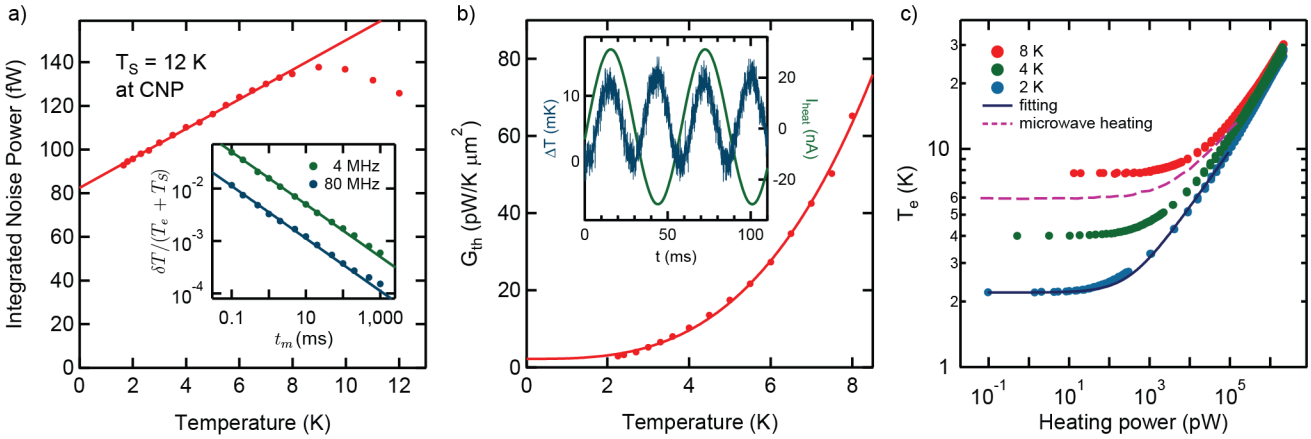

FIG. 2: **A** shows the integrated noise power vs refrigerator temperature, demonstrating the expected temperature dependence of the Johnson noise signal. The deviation at temperatures above 8K due to the temperature dependence of the NbTiN inductor. The inset shows the precision of the noise thermometry taken with two measurement bandwidths, 4 and 80 MHz, vs integration time. A resolution of 100 ppm is achieved, in agreement with the Dicke Radiometer formula (shown as lines). **B** shows the results of the differential thermal conductance measurements. The inset show a time trace, taken at 4 K, of the small heating current at 17.6 Hz, and the resulting 12 mK temperature oscillations at 35.2 Hz detected with the noise thermometer. The red curve is a power law fit with exponent 2.7 ± 0.3. **C** shows the results of applying large dc heating currents at various sample temperatures, T_p (points.) The expected form is shown as the blue line. Also shown, is the heating of the electron gas vs applied microwave power at 1.161 GHz, also showing a similar heating curve and demonstrating the microwave bolometric effect with graphene.

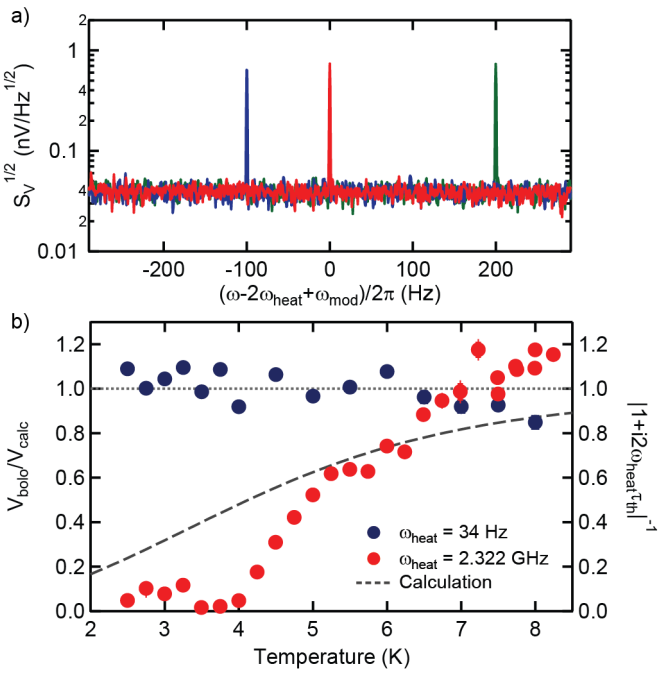

FIG. 3: **A** shows the spectrum, refered to the input of the HEMT, due to bolometric mixing. The central, 600 pV red tone is due to a heating signal at $\omega_{heat}/2\pi = 1.161$ GHz, which produces a temperature response at 2.322 GHz, which is then mixed down to $\omega_{bolo} = \omega_{heat} + 2\pi \cdot 1$ kHz using a small modulation tone at $\omega_{mod} = \omega_{heat} - 2\pi \cdot 1$ kHz. The blue spike, shifted down by 100 Hz, is the result of increasing the modulation tone by 100 Hz. The green spike, shifted up by 200 Hz, is due to increasing the heating tone by 100 Hz, validating the expected relationship: $\omega_{bolo} = 2\omega_{heat} - \omega_{mod}$. **B** shows a plot of the measured bolometric mixing tone normalized by our expected signal assuming the graphene thermal time constant $\tau = 0$. The red points are measured with a heating tone of $\omega_{heat}/2\pi = 1.161$ GHz, and blue points with $\omega_{heat}/2\pi = 17.6$ Hz, both with a modulation tone of 1.161 GHz-1 kHz. The dashed line shows he expected rolloff of the bolometric signal when $2\omega_{heat}/2\pi = 2.32$ GHz and $\tau = C_e/G_{\rm ep}$.

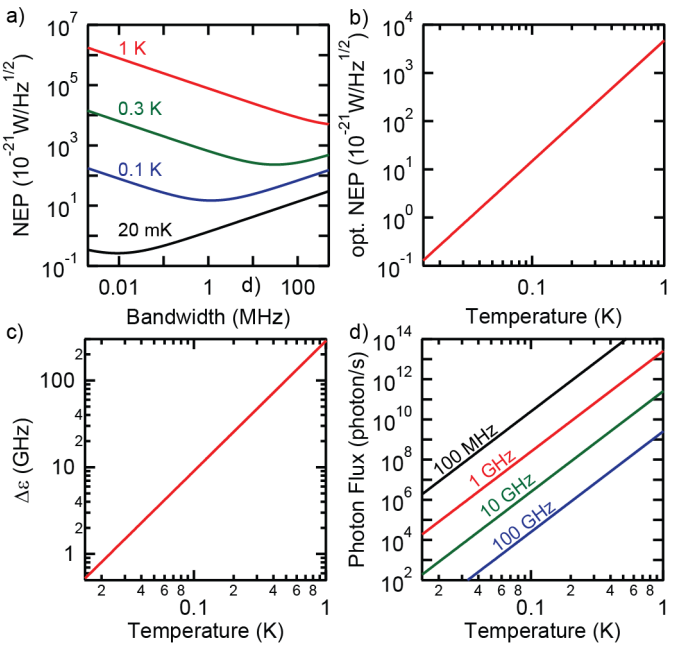

FIG. 4: **A** shows the expected sensitivity as a bolometer assuming $n = 10^9$ cm^2 and $A = 10^{-11}$ m^2 versus coupling bandwidth, for various cryogenic operating temperatures, with **B** showing the optimal value versus temperature. **C** shows the expected energy sensitivity to single photons. **D** shows the threshold for detection of shot noise of an incident microwave field of various frequencies.